International Journal of Mechanics and Applications 2013, 3(4): 88-97
DOI: 10.5923/j.mechanics.20130304.05

PIV Study of a 45° Piched Blade Turbine: Up and Down-Pumping Direction Effect on the Hydrodynamic Structure in a Stirred Tank

Bilel Ben Amira, Zied Driss*, Mohamed Salah Abid

Laboratory of Electro-Mechanic Systems (LASEM), National School of Engineers of Sfax (ENIS), University of Sfax (US), B.P. 1173, Road Soukra km 3.5, Sfax, 3038, Tunisia

Abstract In this paper, we are interested in analysing the hydrodynamic structure of turbulent flow for up- and down-pumping pitched six-blade turbines in which the blade inclination is equal to 45°. Particle image velocimetry (PIV) technique was used to evaluate the distribution of the velocity field, the absolute velocity, the mean instantaneous velocity, the vortices, the turbulent kinetic energy, the dissipation rate of the turbulent kinetic energy and the turbulent viscosity. Experimental results are taken from the vertical measurement plane which is located in the middle of two blades. In this respect, concerning the up-pumping configuration, the volume above the impeller is more extended than in the down-pumping configuration. However, in the down-pumping configuration, the volume below the impeller is more extended than in the up-pumping configuration.

Keywords Pitched Blade Turbines, up, down, Pumping, Turbulent Flow, PIV

1. Introduction

As far as mechanically agitated tank is concerned, impeller geometries have been carried out with experimental and numerical studies. Mechanically agitated tank has been studied over a wide range of laboratory and industrially conditions, in order to improve the agitation energy efficiency. In fact, Ammar et al.[1] used a CFD code "Fluent" to study the effect of the tank design on the hydrodynamic structure in three tanks. Karray et al.[2] developed a specific code to solve the fluid-structure interaction in a mixing vessel equipped with a Rushton turbine. Kchaou et al.[3] used a computational fluid dynamic model to study the hydrodynamic behaviour induced by a flat-blade turbine, and a pitched-blade turbine in a stirred vessel. Aubin et al.[4] used a computational fluid dynamics to estimate the single phase turbulent flow in a stirred tank by a down- and up-pumping pitched blade turbine. Moreover, Bertrand et al.[5] used computational fluid dynamics calculations based on large-eddy simulation (LES) and a sub-grid model of micro-mixing to model the uranium oxalate precipitation for an unbaffled reactor. Linteris et al.[6] used a numerical method to calculate the thermodynamic equilibrium and the perfectly-stirred reactor with detailed reaction kinetics to understand the reasons behind producing the unexpected enhanced combustion. In addition, Roudsari et al.[7] used multiple reference frames (MRF) technique, k–ε model, and Eulerian–Eulerian approach to model the mixing of water in oil emulsion in a lab-scale mixing tank equipped with a Rushton turbine impeller. Falola et al.[8] developed a mathematical model to predict the appearance of the reliably mixing in stirred vessels of a given geometry, and its effect on the crystallization kinetics and crystal product properties. Torop[9] developed an algorithm to estimate the statement of the problem and realization of the probability hazard analysis of safe operation of pipeline systems, tanks, and pressure vessels. Driss et al.[10] developed a specific computational fluid dynamics (CFD) code to predict the turbulent flow in a stirred tank equipped with three pitched blade turbines (PBT). On the other hand, other experimental studies were developed. Thereby, Fontaine et al.[11] used two-dimensional particle image velocimetry (PIV) to evaluate the effect of highly shear - thinning and viscoelastic behaviour on the performance of the mixer equipped with a Max blend, using Newtonian and non-Newtonian fluids in laminar and early transitional regimes. Cole et al.[12] measured the trajectory of tracer particles with positron emission particle tracking (PEPT) in a Rushton stirred vessel. Ben Amira et al.[13] studied the effect of the recorded images in the vessel performance equipped with eight flat blades turbine for a PIV experience. Also, Driss et al.[14] studied the seeding particle mass quantity effect in the PIV measurement in a stirred vessel

* Corresponding author:
zied.driss@enis.rnu.tn (Zied Driss)
Published online at http://journal.sapub.org/mechanics

equipped by a Rushton turbine. Li et al.[15] used the PIV technique to calculate the velocity field generated by a Rushton turbine. Driss et al.[16] used 2D PIV technique to study the turbulent flow inside a cylindrical baffled stirred vessel with a set of speed that was selected ranging from 100 rpm to 350 rpm. Escudié and Liné[17] used two-dimensional PIV technique to analyze the different types of hydrodynamics that coexist in the tank equipped with a Rushton turbine. Ben Amira et al.[18] studied the blade inclination effect of three different turbines characterised by the inclination angles equals to β=45°, β=60° and β=75°. Houcine et al.[19] described the mixing in a tank equipped with different agitation devices (Rushton turbine and mixed TTP propeller) with a very low power input, by means of the laser induced fluorescence technique. Guillard et al.[20] used Laser Induced Fluorescence (PLIF) to investigate the turbulent mixing process in a model stirred tank equipped with two Rushton turbines of standard geometry. Kawase et al.[21] studied the laminar boundary-layer heat transfer in a stirred tank with non-Newtonian fluids, experimentally and theoretically.

Relying on these results, the study of the blade geometric is important to ameliorate the efficiently of the tank. Thereby, 45° pitched blade turbine is proposed for the up and down configurations.

2. Experiment Device

The schematic illustration of experimental apparatus was shown in figure 1. The characterization of the hydrodynamic structure of the turbulent flow in our experience was provided by a two dimensional particle image velocimetry system (PIV). Thus, the PIV system consists of a Nd:YAG laser equipped with double cavity, and producing a green beam at 532 nm wave length. Each cavity produces a 30 mJ of energy, whereas, the successive pairs of pulses were separated by 200 µs. The images are recorded through a high dynamic 14 bit cooled CCD camera system with a resolution of 1600 x 1200 and a clock frequency equal to 1.6 GHz. The CCD camera is equipped with an integrated image memory (cam RAM) into the camera itself (512 MB), and enables unmatched fast image recording with 160 MB.s^{-1}. The synchronization between the different PIV components is controlled by a mini-synchronizer. This device is composed of a 16 bits micro-controller operating at 25 MHz and minimum time resolution for all signals equal to 40 ns. In addition, the mean diameter of the Polyamide microspheres particles is equal to 20 µm, and their mass quantity is equal to 0.15 g inside the whole vessel volume. An electrical motor is mounted above the vessel to maintain the movement of the turbine. As shown in figure 2, the experimental study consists of the up- and down-pumping pitched six-blade turbines in which the blade inclination is equal to 45° (45° PBTU and 45° PBTD). The diameter of the impeller is equal to d=100 mm. The turbine was mounted in axial position equal to c=100 mm from the bottom of the tank. In addition, the height of the vessel is taken equal to its diameter (H=D=300 mm).

Figure 1. Experimental apparatus

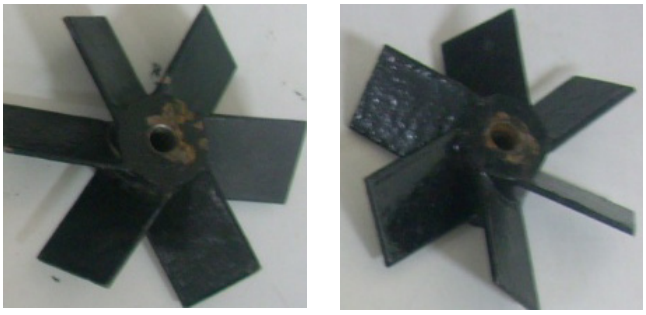

(a) 45° PBTU (b) 45° PBTD

Figure 2. Up and down pumping 45° pitched six blade turbines

3. Results

The experimental results were presented in the azimuthally plane which is located in the middle of two blades. In this respect, the tangential velocity at the tip of the blade is equal to V_{tip}=0.8 m.s^{-1}. The Reynolds number is equal to Re=26010.

3.1. Velocity Field

Figure 3 shows the velocity field for both the 45° PBTU and 45° PBTD. Therefore, the velocity in the main recirculation loop- near or far the impeller- does not exceed 45 % of the U_{tip} maximum and 0.075 % of the U_{tip} minimum. In fact, two different zones are presented. The first zone is in the levels of the z higher than the impeller, and the second, in the z lower than the impeller. In fact, one of these zones is characterized by the vortices attached to the blade and the passage of the vortices from the previous blade. However, the other zone is characterized with the absence of vortices. Obviously, in the up-pumping configuration, the volume above the impeller is more extended than in the down - pumping configuration. However, in the down-pumping, the

volume below the impeller is more extended than in the up - pumping configuration. In this case, two main recirculation loops are presented in the up-pumping configuration in which one is localized in the third upper zone of the vessel close to the free surface and the second is localized in the middle zone near the wall of the vessel. Nevertheless, there are no vortices presented in the bottom of the vessel which has the lowest velocity. However, one main circulation loop is presented in the down-pumping configuration, and localized in the bottom of the vessel and near the vessel wall. In addition, there are no vortices presented in the volume above the impeller with the lowest velocity.

Close to the impeller, the stream discharged from the blade causing a local velocity in the up - pumping configuration. Whereas, the velocity increases as the fluid accelerates from a downward to an upward direction in the upper reaches of the vessel. In fact, the sloping stream turns vertically close to the impeller. Then, velocity direction becomes vertically upward and downward along the side wall. On the other hand, for the down-pumping configuration, the velocity increases as the fluid accelerates from an upward to a downward direction in the inferior part of the vessel. In fact, the sloping stream turns vertically close to the impeller, then, confined by the bottom wall. It turns horizontally, and, then, moves vertically upward along the side wall.

In addition, considering the up-pumping configuration, the highest values of velocity are in the impeller discharge region in which U_{max}=27.4 % V_{tip} and U_{moy}=4.49 % V_{tip}. A similar situation has been observed in the down-pumping configuration, whilst U_{max}=44.7 % V_{tip} and U_{moy}=4.51 % V_{tip}. Consequently, the velocity in the down-pumping configuration is greater than the velocity in the up-pumping configuration. The secondary flow is generated due to the gravity force. Furthermore, this phenomenon can be clearly observed in the other zones of the vessel, whilst they are less affected by the flow loop and relatively quiescent, with velocities of 0.075 % V_{tip}.

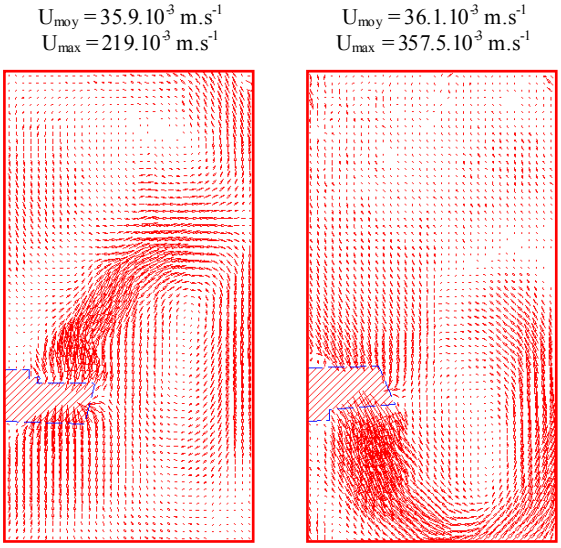

Figure 3. Velocity field

3.2. Absolute Velocity

Figure 4 shows the distribution of the absolute velocity for both the 45° PBTU and 45° PBTD. Therefore, the region with the high value is located in the same direction of the stream discharge. In fact, the area with the highest values is presented between the two main recirculation loops for the up-pumping turbine. Furthermore, this area is localized in the bottom of the tank for the down-pumping turbine. In addition, the velocity value decreases as it goes away from the blade.

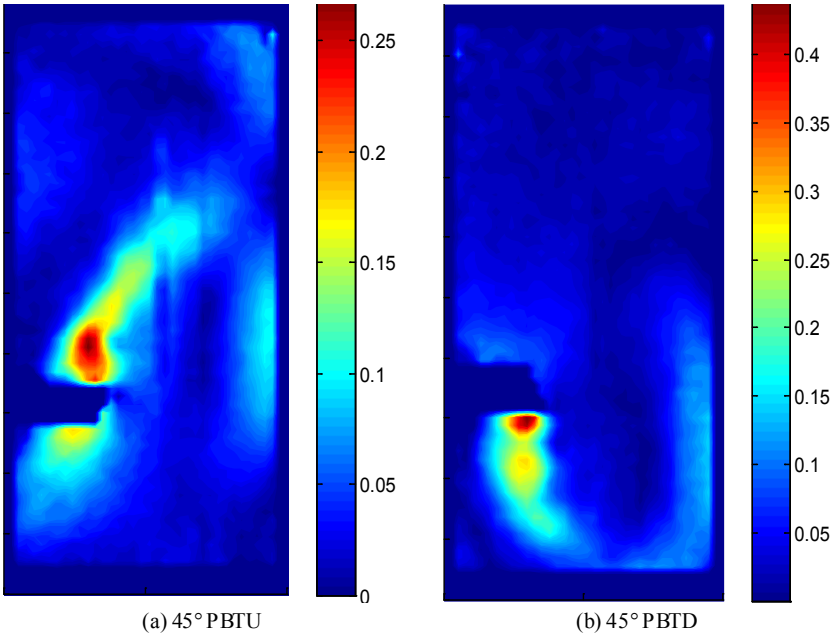

Figure 4. Absolute velocity

3.3. Absolute rms Velocity

Figure 5 shows the distribution of the absolute rms velocity for both the 45° PBTU and 45° PBTD. Similarly, as the absolute velocity, the region with the high value is located in the same direction of the stream discharge. In fact, the area with the highest values is presented between the two main recirculation loops for the up-pumping turbine. Furthermore, this area is localized in the bottom of the tank for the down-pumping turbine. In addition, the velocity value decreases as it goes away from the blade. Moreover, the absolute rms velocity areas are larger than the absolute velocity areas.

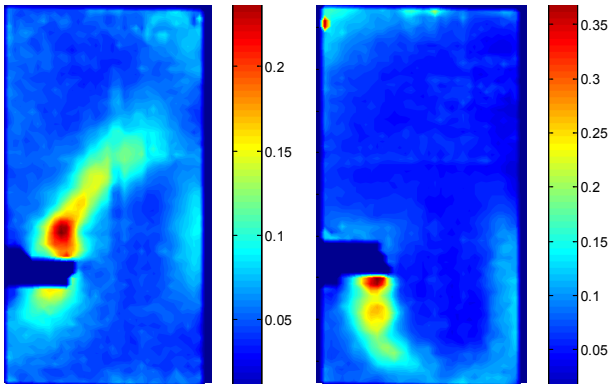

(a) 45° PBTU (b) 45° PBTD

Figure 5. Absolute rms velocity

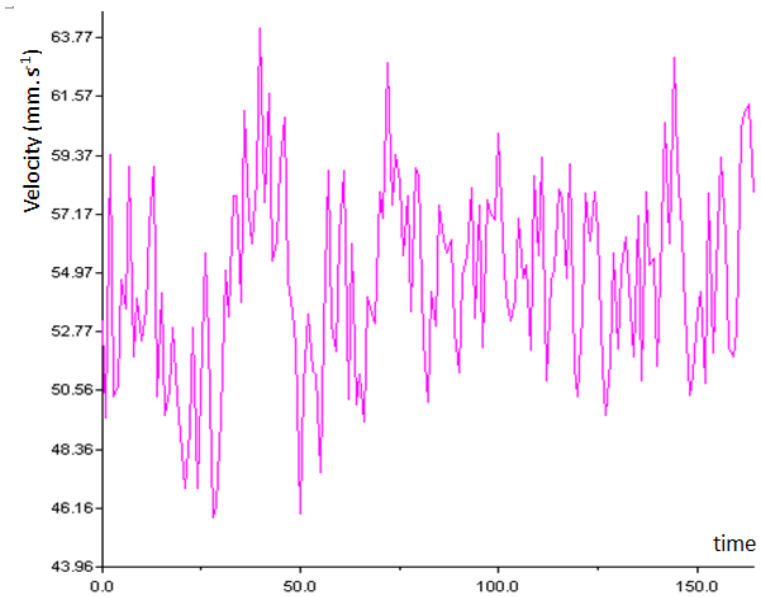

(a) 45° PBTU

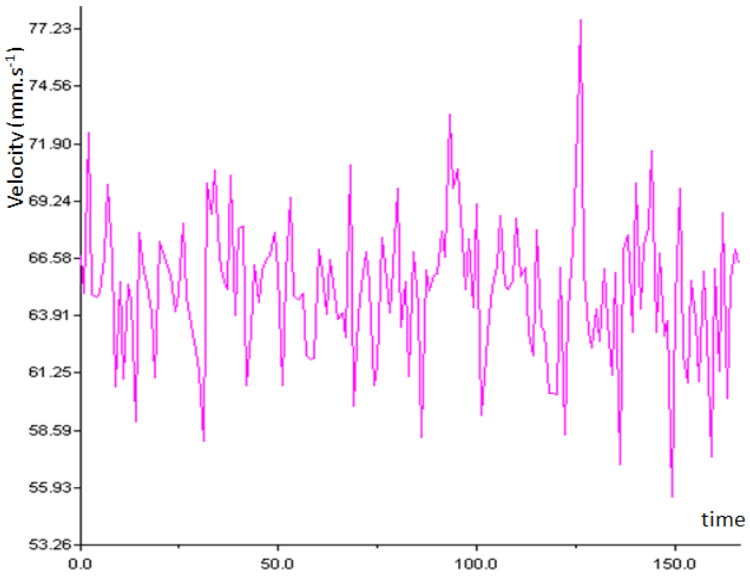

(b) 45° PBTD

Figure 6. Variation of the mean instantaneous velocity with time

3.4. Mean Instantaneous Velocity

Figure 6 shows the variation of the mean instantaneous velocity with time, for, both, the 45° PBTU and 45° PBTD. Subsequently, for the two applications, the x-axis presents the time axis in which the unit of time reflects to one shaft rotation which represents one acquisition of the paired images. Therefore, the shaft takes 0.4 second for one turn. Thereby, it is clear that the flow oscillates in a sinusoidal form-in which the highest fluctuation represents the top of the main oscillation. Furthermore, it is shown that the fluctuation interval of the mean velocity in the down-pumping configuration is greater than that in up-pumping configuration. The interval of the mean velocity in the down-pumping configuration is equal to $\Delta V=22.3\ 10^{-3}$ $m.s^{-1}$, whereas, the mean velocity in the up-pumping configuration is equal to $\Delta V=18.5\ 10^{-3}$ $m.s^{-1}$. In this context, it is shown that ΔV is greater at the beginning of the experience, and it decreases at the end, for up-pumping configuration. However, ΔV is lower at the beginning of the experience and it increases at the end, for down-pumping configuration.

3.5. Vorticity

Figure 7 shows the distribution of the vorticity for both the 45° PBTU and 45° PBTD. It presents the trailing vortices from the blade to the bulk region of the tank. In fact, the maximum values are observed in two locations corresponding to the location of highest value and the lowest values for both up- and down-pumping configurations. Consequently, the highest and lowest local vortices values were found at the impeller level, and they become medium moving both upward and downward from this level. In addition, the furthest regions away from the impeller are obtained due to the vortex generated by the previous blade. Thereby, the area of the highest values is larger than that of the lowest values, in the up-pumping configuration. Hence, the highest vortices values become larger and more diffuse in the bulk of the discharge flow. But the area of the lowest value is more distinct and localized at the upper reaches of the impeller. Indeed, it has been observed that the value of the highest vortices is much lower than the absolute lowest vortices value. On the other hand, the highest vortices values are presented in two different areas in the down- pumping configuration. Thereby, the area of the highest values is more distinct, and localized downer the impeller than that of the lowest values. In fact, the down-pumping turbine transfers the vortex at lowest values to the region near the bottom of the tank, then, it is diffused in the bulk of the discharge flow. Also, it has been observed that the value of the highest vortices is much higher than the absolute lowest vortices value. Afterward, it has been noted that the vortices high value of the down-pumping configuration is greater than the vortices high value of the up-pumping configuration. However, the absolute value of the lowest vortices of the down-pumping configuration is lower than the absolute value of the lowest vortices of the up-pumping configuration.

3.6. Shear Strain

Figure 8 shows the distribution of the shear strain for both the 45° PBTU and 45° PBTD. Therefore, tow maximum areas were presented. The first area represents the highest values and the second area represents the lowest values. In fact, the maximum areas are localized close to the blade in the same direction of the stream discharge. The bulk region of the tank is presented with the medium value. Furthermore, the down-pitched blade turbine is described with the highest shear strain values.

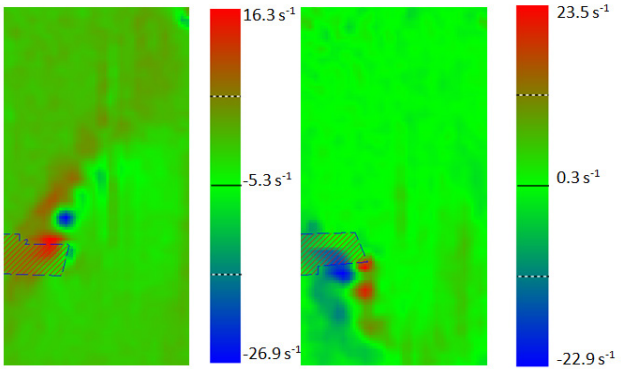

(a) 45° PBTU (b) 45° PBTD

Figure 7. Vortices

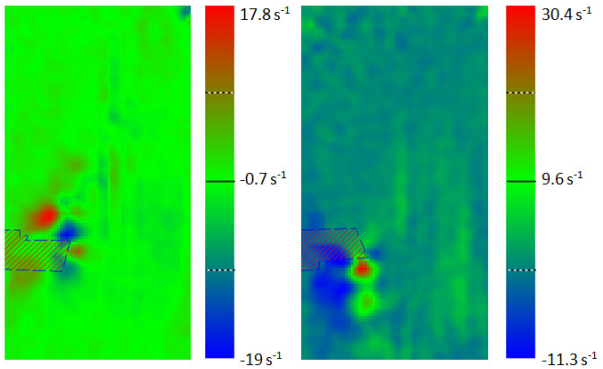

(a) 45° PBTU (b) 45° PBTD

Figure 8. Shear Strain

3.7. Turbulent Kinetic Energy

Figure 9 shows the distribution of the turbulent kinetic energy for both the 45° PBTU and 45° PBTD. The transportation of the turbulent kinetic energy is consistent with the movement of the trailing vortices, which results in energy transfer from the blade to the bulk region of the tank. Generally, the region with high turbulent kinetic energy is located in the interaction area of the trailing vortices. In addition, the regions furthest away from the impeller are obtained due to the vortices generated by the previous blade. Consequently, the turbulent kinetic energy in the up -pumping configuration has two maximum regions. The first is localized in the inferior area of the impeller, and, the second, in the upper area of the impeller. In fact, the faraway

region is localized in the same direction of the velocity acceleration, between the two main circulation loops. However, the narrowest area is localized close to the impeller due to the absence of the vortices. Furthermore, there is an overlap between the areas of maximum turbulent kinetic energy, but, they become larger and more diffuse in the bulk of the discharge flow. The rest of the bulk region of the tank has the lowest values of the turbulent kinetic energy. However, it is clear that the regions of the high turbulent kinetic energy in the down-pumping configuration are more distinct. In fact, the down-pumping turbine transfers the turbulent kinetic energy to the region near the bottom of the tank. Therefore, in this case, it has been observed that the turbulent kinetic energy region which is generated with one main circulation loop is different from the one in the double main circulation loops which are transferred to the upper-right region of the turbine. Furthermore, the region of high turbulent kinetic energy is diffused in the bulk of the discharge flow. Afterward, it has been observed that the high turbulent kinetic energy value of the down-pumping configuration is greater than the high turbulent kinetic energy value of the up-pumping configuration.

3.8. Dissipation Rate of the Turbulent Kinetic Energy

Figure 10 shows the dissipation rate of the turbulent kinetic energy for both the 45° PBTU and 45° PBTD. In fact, the region with high dissipation rate of the turbulent kinetic energy is located in the interaction area of the trailing vortices. In addition, the regions furthest away from the impeller are obtained due to the vortex generated by the previous blade. Consequently, the dissipation rate of the turbulent kinetic energy in the up-pumping configuration has two distanced areas. One of these areas is localized below the impeller, and, the second one is localized above the impeller. In fact, the faraway region is localized in the same direction of the velocity acceleration, between the two main circulation loops, and it represents the largest area. However, the narrowest area is localized close to the impeller due to the absence of the vortices. Furthermore, two areas of maximum dissipation rate of the turbulent kinetic energy have been observed with some overlap, above the impeller. Thus, they become larger and more diffuse in the bulk of the discharge flow. The rest of the bulk region of the tank has the lowest values. However, it is clear that the regions of high dissipation rate of the turbulent kinetic energy in the down-pumping configuration are more distinct and localized. In fact, the down-pumping turbine transfers the energy to the region near the bottom of the tank. Furthermore, the region of high dissipation rate of the turbulent kinetic energy is diffused in the bulk of the discharge flow. Therefore, it has been observed that the regions which are generated with one main circulation loop are different from the one in the double main circulation loops. In addition, a second maximum region is presented on the left of the tank, near the shaft and the free surface, due to the reflection. Afterward, it has been observed that the high dissipation rate of the turbulent kinetic energy value of the down-pumping configuration is greater than the up-pumping configuration.

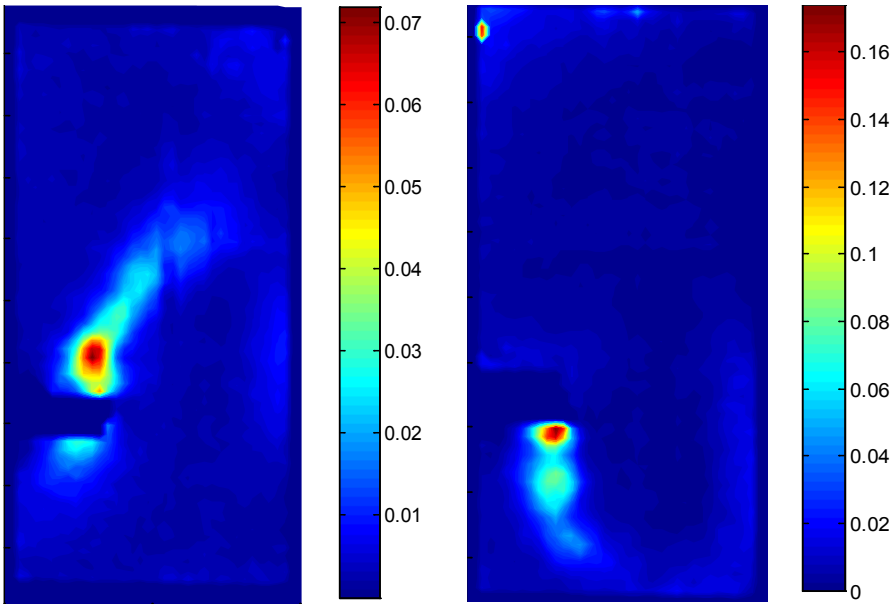

(a) 45° PBTU (b) 45° PBTD

Figure 9. Turbulent kinetic energy

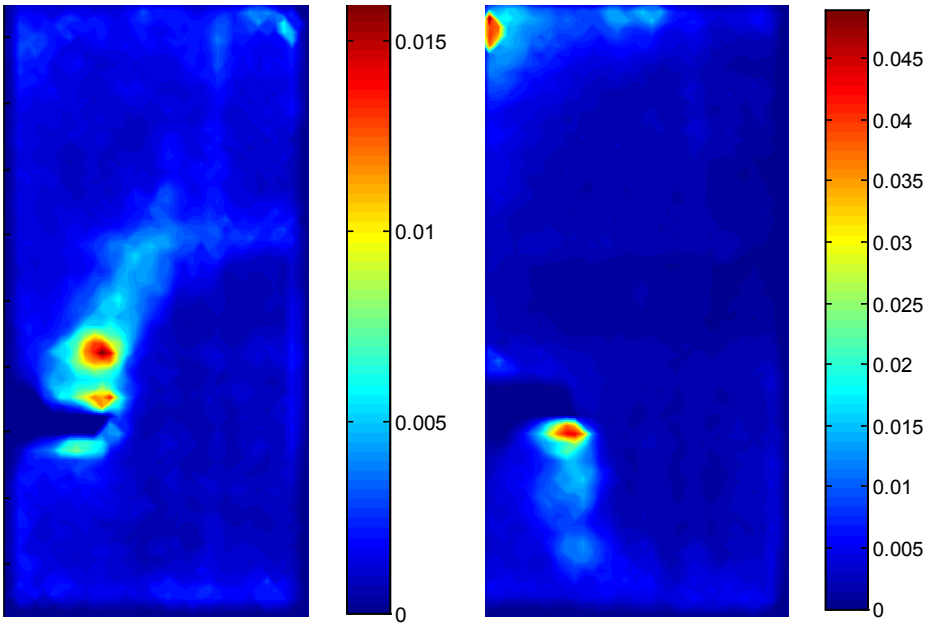

(a) 45° PBTU (b) 45° PBTD

Figure 10. Dissipation rate of the turbulent kinetic energy

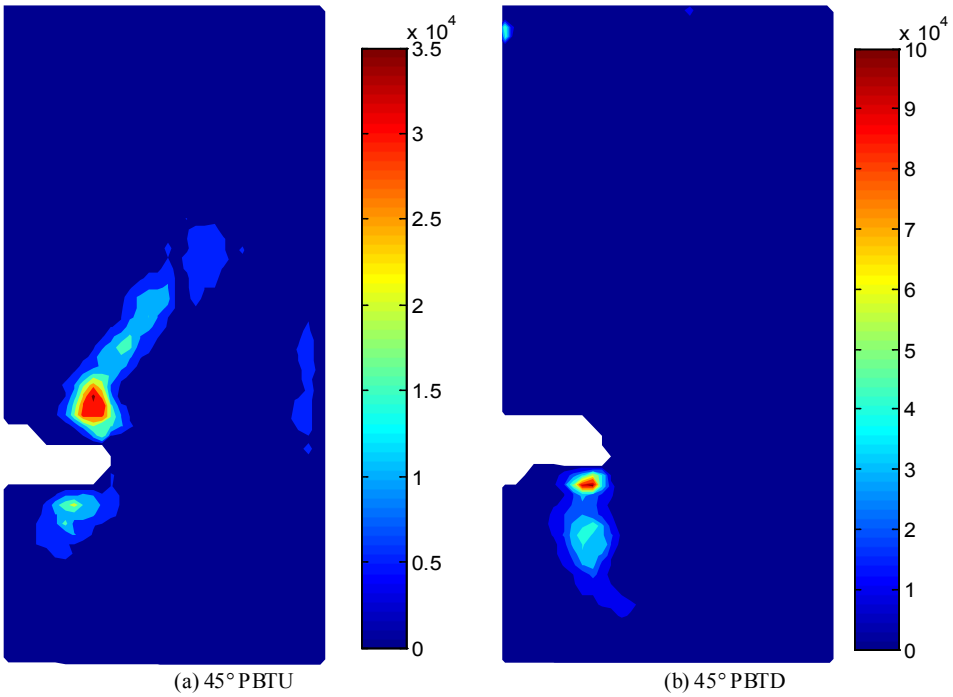

(a) 45° PBTU (b) 45° PBTD

Figure 11. Turbulent viscosity

3.9. Turbulent Viscosity

Figure 11 shows the distribution of the turbulent viscosity for both the 45° PBTU and 45° PBTD. In fact, the transportation of the turbulent viscosity is consistent with the movement of the trailing vortices, which results in energy transfer from the blade to the bulk region of the tank. Therefore, the turbulent viscosity in the up-pumping configuration has two maximum regions. One of these areas is below the impeller, and, the second one is above the impeller. Generally, these regions -with high turbulent viscosity- are located in the interaction area of the trailing vortices. In fact, the faraway region is localized in the same direction of the velocity acceleration, between the two main circulation loops. Furthermore, the areas of high turbulent viscosity have been observed with some overlap. Then, they become larger and more diffuse in the bulk of the discharge flow. However, the narrowest area is below the turbine, close to the impeller. In this respect, the regions of high turbulent viscosity in the down-pumping configuration are more

distinct and localized. In fact, the down-pumping turbine transfers the turbulent kinetic energy to the region near the bottom of the tank. Furthermore, the region of high turbulent viscosity is diffused in the bulk of the discharge flow. In addition, the rest of the bulk region of the tank has the lowest values of turbulent viscosity, for both up- and down - pumping configurations. Afterward, it has been observed that the highest turbulent viscosity value (μ_t=105465) of the down-pumping configuration is greater than the highest turbulent viscosity value of the up-pumping configuration (μ_t=36994).

3.10. Turbulent Intensity

Figure 12 shows the distribution of the turbulent kinetic energy for both the 45° PBTU and 45° PBTD. In fact, areas with the highest value are distinct and spread in the bulk region of the vessel. In addition, it is clear that the flow generated by the down-pitched blade is more intense than the flow generated by the up-pitched blade turbine.

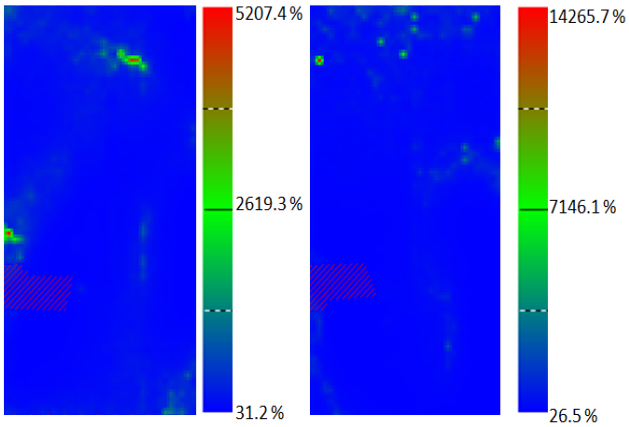

(a) 45° PBTU (b) 45° PBTD

Figure 12. Turbulent intensity

3.11. Profiles

Figures 13, 14, 15, 16 and 17 report the radial profiles of the velocity field and the turbulent characteristics. These results are plotted in axial positions equal to z/H=1.5. In fact, the radial profile of the axial velocities is displayed in figure 13. Therefore, it has been observed that the axial velocity of the 45° PBTU is positive, near the shaft, and, decreases near the tank wall. However, for the 45° PBTD the axial velocity is positive, near the shaft, and, increases near the tank wall, as a sinusoidal trajectory. Radial vorticity profiles are shown in figure 14. In fact, for the 45° PBTU the vorticity issued with a sinusoidal trajectory which dampens moving away from the shaft. Nevertheless, the reverse phenomenon is produced for the 45° PBTD. Moreover, for the radial distribution of the normalized turbulent kinetic energy, both up and down configurations have the same value near the wall of the tank (figure 15). However, the up configuration is greater than the down configuration at the other radial positions. Figure 16 shows the radial distribution of the normalized dissipation rate of the turbulent kinetic energy. Therefore, it has been observed that the up and the down configurations have a similar distribution, whilst the up configuration is greater than the down configuration. Actually, figure 17 illustrates the radial profile of the normalized turbulent viscosity distribution. Results show that a Gaussian distribution is presented in the up - configuration. Furthermore, the maximum pick is localized near the shaft for the up-configuration, and near the vessel wall for the down one.

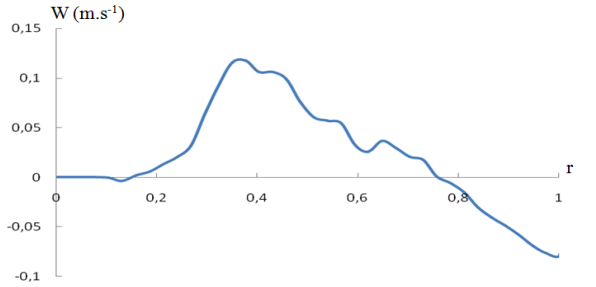

(a) 45° PBTU

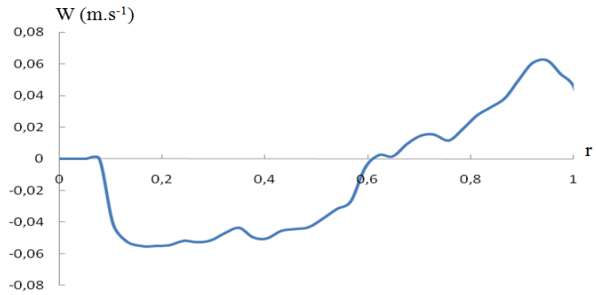

(b) 45° PBTD

Figure 13. Radial profile of the axial velocity (W=f(r))

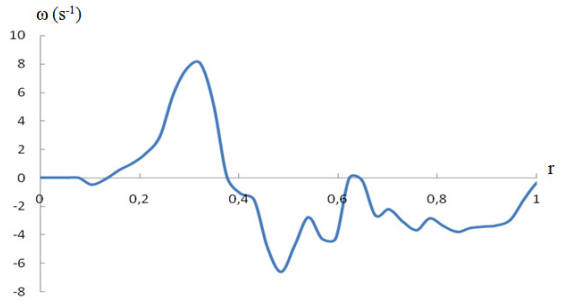

(a) 45° PBTU

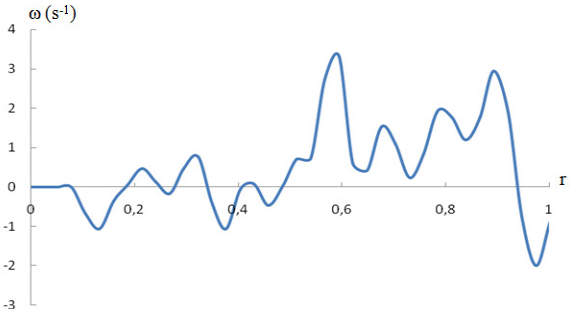

(b) 45° PBTD

Figure 14. Vorticity radial profiles (ω=f(r))

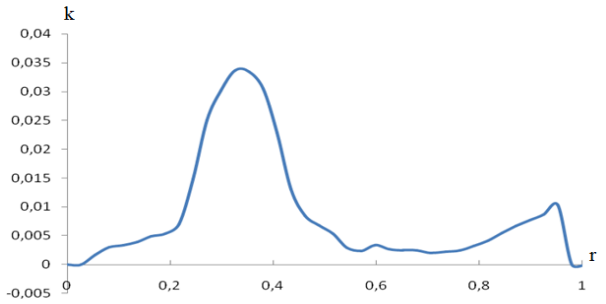

(a) 45° PBTU

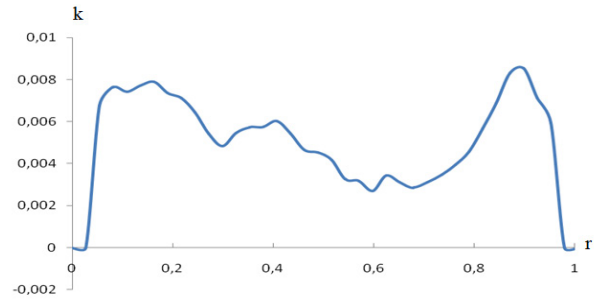

(b) 45° PBTD

Figure 15. Normalized radial profile of the turbulent kinetic energy (k=f(r))

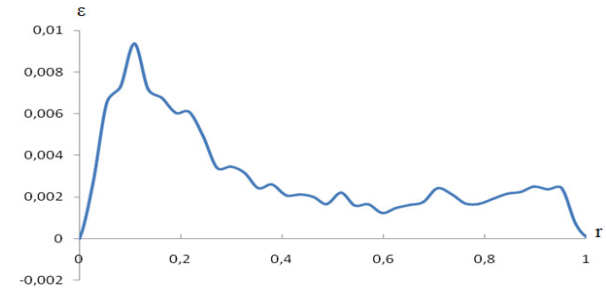

(a) 45° PBTU

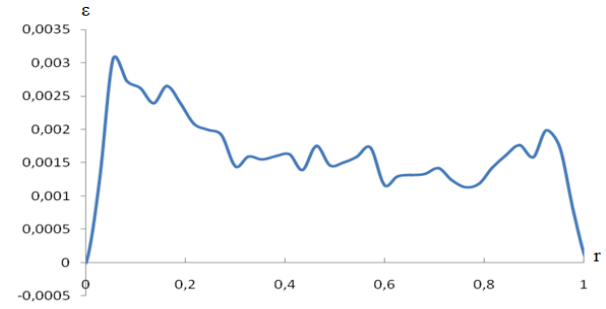

(b) 45° PBTD

Figure 16. Normalized radial profile of the dissipation rate of the turbulent kinetic energy (ε=f(r))

4. Conclusions

This paper focuses on the experimental study of the pumping direction effect of the 45° up- and down-pitched blades turbines. Several results are presented to modulate the vessel for each blade configuration. In fact, it is shown that for the up-configuration the vessel is more agitated near the shaft. However, it is more agitated near the tank wall for the down configuration. In fact, in the up-pumping configuration, the volume above the impeller is more extended than in the down-pumping configuration. However, in the down - pumping, the volume below the impeller is more extended than in the up-pumping configuration. In this case, two main circulation loops are presented in the up - pumping configuration. One main circulation loop is presented in the down-pumping configuration, and is localized in the bottom of the vessel, near the vessel wall. These results explain the difference between the up and the down 45°-pitched blade turbines. In the future, other configurations will be proposed by the means of the stereoscopic particle image velocimetry (PIV).

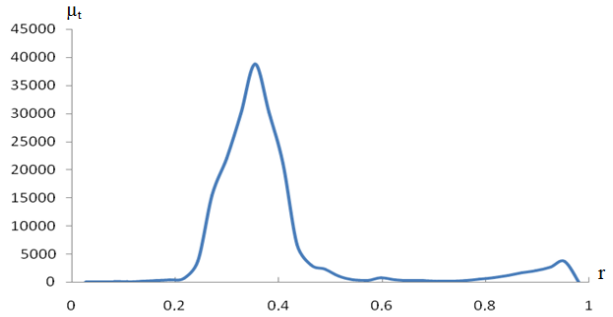

(a) 45° PBTU

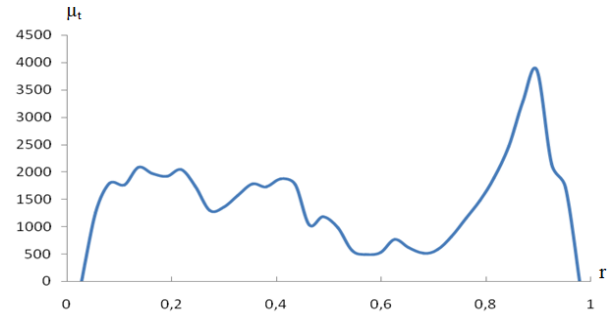

(b) 45° PBTD

Figure 17. Normalized radial profile of the turbulent viscosity (μ_t=f(r))

Nomenclature

d	diameter of the impeller (mm).
c	turbine is axial position (mm).
H	vessel height (mm).
D	vessel diameter (mm).
Re	Reynolds number (dimensionless).
N	Shaft speed (rpm).
W	axial velocity (ms^{-1}).
V_{tip}	tangential velocity at the blade tip ($m.s^{-1}$).
ΔV	interval of the mean velocity ($m.s^{-1}$).
U_{moy}	mean velocity ($m.s^{-1}$).
U_{max}	maximum velocity ($m.s^{-1}$).
ω	Vortices (s^{-1}).
$\varepsilon^* = \frac{\varepsilon}{(2\pi N)^3 (d/2)^2}$	dissipation rate of the turbulent kinetic energy (dimensionless).
$k^* = \frac{k}{(\pi N d)^2}$	turbulent kinetic energy (dimensionless).
μ_t	turbulent viscosity (dimensionless).

REFERENCES

[1] M. Ammar, Z. Driss, W. Chtourou, and M. S. Abid, "Effect of the Tank Design on the Flow Pattern Generated with a Pitched Blade Turbine", International Journal of Mechanics and Applications, Vol. 2, N. 1, pp. 12-19, 2012.

[2] S. Karray, Z. Driss, A. Kaffel, H. Kchaou, M. S. Abid, "Fluid-structure interaction in a stirred vessel equipped with the Rushton turbine, International Journal of Mechanics and Applications", Vol. 2, N. 6, pp. 129-139, 2012.

[3] H. Kchaou, Z. Driss, G. Bouzgarrou, W. Chtourou, M. S. Abid, "Numerical Investigation of Internal Turbulent Flow Generated By A Flat-Blade Turbine and A Pitched-Blade Turbine in A Vessel Tank", International Review of Mechanical Engineering (I.RE.M.E.), Vol. 2, N. 3, 2008.

[4] J. Aubin, D.F. Fletcher, C. Xuereb, "Modeling turbulent flow in stirred tanks with CFD: the influence of the modeling approach, turbulence model and numerical scheme", Experimental Thermal and Fluid Science Vol. 28, pp. 431-445, 2004.

[5] M. Bertrand, E. Plasari, O. Lebaigue, P. Baron, N. Lamarque, F. Ducros, "Hybrid LES–multizonal modelling of the uranium oxalate precipitation", Chemical Engineering Science Vol. 77, pp. 95-104, 2012.

[6] G. T. Linteris, D. R. Burgess, F. Takahashi, V. R. Katta, H. K. Chelliah, O. Meier, " Stirred reactor calculations to understand unwanted combustion enhancement by potential halon replacements", Combustion and Flame Vol. 159, pp. 1016–1025, 2012.

[7] S. F. Roudsari, G. Turcotte, R. Dhib, F. Ein-Mozaffari, "CFD modeling of the mixing of water in oil emulsions", Computers and Chemical Engineering Vol. 45, pp. 124-136, 2012.

[8] A. Falola, A. Borissova, c. Sim, A software environment for modelling industrial batch cooling Crystallization, Computers and Chemical Engineering Vol. 38, pp. 35-43, 2012.

[9] V. M. Torop, "Probability hazard analysis of the operation of pipeline systems, tanks, and pressure vessels. part 1 algorithm of construction of the probability model", Strength of Materials, Vol. 37, pp. 174-179, 2005.

[10] Z. Driss, G. Bouzgarrou, W. Chtourou, H. Kchaou, M.S. Abid, "Computational studies of the pitched blade turbines design effect on the stirred tank flow characteristics", European Journal of Mechanics B/Fluids Vol. 29, pp. 236-245, 2010.

[11] A. Fontaine, Y. Guntzburger, F. Bertrand, L. Fradette, M.-C. Heuzey, "Experimental investigation of the flow dynamics of rheologically complex fluids in a Maxblend impeller system using PIV", Chemical engineering research and design Vol. 91, pp. 7-17, 2013.

[12] K.E. Cole, A. Buffler, N.P.V. Meulen, J.J. Cilliers, J.P. Franzidis, I. Govender, C. Liu, M. R. van Heerden, "Positron emission particle tracking measurements with 50 micron tracers", Chemical Engineering Science Vol. 75, pp. 235–242, 2012.

[13] B. Ben Amira, Z. Driss, A. Kaffel, S. Karray, M. S. Abid, "Etude de l'influence du nombre d'images sur les résultats obtenues a l'aide d'un système PIV appliquée a une turbine a huit pales droites", 2ème Conférence Maghrébine sur les Matériaux et l'énergie, 2012.

[14] Z. Li, Y. Bao, Z. Gao, "PIV experiments and large eddy simulations of single-loop flow fields in Rushton turbine stirred tanks", Chemical Engineering Science, Vol. 66, pp. 1219-1231, 2011.

[15] Z. Driss, A. Kaffel, B. Ben Amira, G. Bouzgarrou, M.S. Abid, "PIV measurements to study the effect of the Reynolds number on the hydrodynamic structure in a baffled vessel stirred by a Rushton turbine", Science Academy Transactions on Renewable Energy Systems Engineering and Technology (SATRESET), Vol. 2, No. 4, 2046-6404, 2012.

[16] Z. Driss, G. Bouzgarrou, A. Kaffel, M.S. Abid, "Experimental Study of the Seeding Mass Quantity Effect on the PIV Measurements Applied on a Stirred Vessel Equipped by a Rushton Turbine", International Journal of Mechanics and Applications, Vol. 2, N. 5, pp. 93-97, 2012.

[17] R. Escudié, A. Liné, "Experimental Analysis of Hydrodynamics in a Radially Agitated Tank", AIChE, Vol. 49, No. 3, 2003.

[18] B. Ben Amira, Z. Driss, S. Karray, M.S. Abid, "PIV study of the down-pitched blade turbine hydrodynamic structure", Proceedings of the Fifth International Conference Design and Modeling of Mechanical Systems, CMSM´2013, Book Part III, 29, 237-244, 2013.

[19] I. Houcine, H. Vivier, E. Plasari, R. David, J. Villermaux, "Planar laser induced fluorescence technique for measurements of concentration fields in continuous stirred reactors", Exp Fluids, Vol. 22, pp. 95-102, 1996.

[20] F. Guillard, C. TraKgasrdh, L. Fuchs, "A study of turbulent mixing in a turbine-agitated tank using a fluorescence Technique", Experiments in Fluids, Vol. 28, No. 225-235, 2000.

[21] Y. Kawase, M. Hoshino, T. Takahashi, "Non-Newtonian laminar boundary-layer heat transfer in stirred tanks", Heat and mass transfer, Vol. 38, pp. 679-689, 2002.